

## Solitonic lattice and Yukawa forces in the rare-earth orthoferrite $\text{TbFeO}_3$

Sergey Artyukhin,<sup>1</sup> Maxim Mostovoy,<sup>1</sup> Niels Paduraru Jensen,<sup>2</sup> Duc Le,<sup>3</sup> Karel Prokes,<sup>3</sup> Vinícius G. Paula,<sup>3,4</sup> Heloisa N. Bordallo,<sup>3,5,6</sup> Andrey Maljuk,<sup>3,7</sup> Sven Landsgesell,<sup>3</sup> Hanjo Ryll,<sup>3</sup> Bastian Klemke,<sup>3</sup> Sebastian Paeckel,<sup>3</sup> Klaus Kiefer,<sup>3</sup> Kim Lefmann,<sup>5</sup> Luise Theil Kuhn,<sup>2,6</sup> and Dimitri N. Argyriou<sup>3,6,8</sup>

<sup>1</sup>*Zernike Institute for Advanced Materials,  
University of Groningen, Nijenborgh 4,  
9747 AG, Groningen, The Netherlands*

<sup>2</sup>*Risø National Laboratory for Sustainable Energy,  
Frederiksborgvej 399, DK-4000 Roskilde, Denmark*

<sup>3</sup>*Helmholtz-Zentrum Berlin für Materialien und Energie,  
Hahn-Meitner Platz 1, D-14109, Berlin, Germany*

<sup>4</sup>*Instituto de Física, Universidade do Estado do Rio de Janeiro,  
Rio de Janeiro, RJ 20559-900, Brazil*

<sup>5</sup>*Nanoscience Center, Niels Bohr Institute,  
University of Copenhagen, DK-2100 Copenhagen, Denmark*

<sup>6</sup>*European Spallation Source ESS AB,  
P.O. Box 176, SE-221 00 Lund, Sweden*

<sup>7</sup>*Leibniz Institute for Solid State and Materials Research Dresden,  
Helmholtzstrasse 20, 01069 Dresden, Germany*

<sup>8</sup>*Department of Synchrotron Radiation Research,  
Lund University, Box 118, Lund, Sweden*

(Dated: April 25, 2012)

I. SYMMETRY ANALYSIS

We use the so-called Bertaut's notations<sup>18</sup> to describe the symmetry of magnetic states of TbFeO<sub>3</sub> (see Table I). The ordering of Fe spins in the HT phase is described by the  $\Gamma_4$  representation. In the IT state both Fe and Tb spin orders have  $\Gamma_2$  symmetry, while in the LT phase the Fe order changes back to  $\Gamma_4$ , while the ordering of Tb spins has  $\Gamma_8$  symmetry (see Fig. 1). Furthermore, the Lifshitz invariant has the form

$$\Gamma_8 \partial_y \Gamma_2 - \Gamma_2 \partial_y \Gamma_8, \quad (1)$$

from which Eq.(4) follows. We note that the rotationally symmetric scalar products,

$$\mathbf{A}' \cdot \partial_y \mathbf{F} - \mathbf{F} \cdot \partial_y \mathbf{A}' \quad \text{and} \quad \mathbf{G}' \cdot \partial_y \mathbf{C} - \mathbf{C} \cdot \partial_y \mathbf{G}', \quad (2)$$

where e.g.  $\mathbf{A}' \cdot \partial_y \mathbf{F} = A'_x \cdot \partial_y F_x + A'_y \cdot \partial_y F_y + A'_z \cdot \partial_y F_z$ , are also invariant under all transformations of the *Pbnm* group showing that the coupling between inhomogeneous rare earth and transition metal magnetic orders can originate from Heisenberg exchange interactions<sup>9</sup>.

	Fe	Tb	$\tilde{m}_x$	$\tilde{m}_y$	$m_z$
$\Gamma_1$	$A_x G_y C_z$	$C'_z$	+	+	+
$\Gamma_2$	$F_x C_y G_z$	$F'_x C'_y$	+	-	-
$\Gamma_3$	$C_x F_y A_z$	$C'_x F'_y$	-	+	-
$\Gamma_4$	$G_x A_y F_z$	$F'_z$	-	-	+
$\Gamma_5$		$G'_x A'_y$	-	-	-
$\Gamma_6$		$A'_z$	-	+	+
$\Gamma_7$		$G'_z$	+	-	+
$\Gamma_8$		$A'_x G'_y$	+	+	-

TABLE I: Transformation properties of representations of *Pbnm* space group under the three generators of the group: the two glide mirrors,  $\tilde{m}_x : (x, y, z) \rightarrow (1/2 - x, 1/2 + y, z)$  and  $\tilde{m}_y : (x, y, z) \rightarrow (1/2 + x, 1/2 - y, 1/2 + z)$ , and the mirror  $m_z : (x, y, z) \rightarrow (x, y, 1/2 - z)$ .

## II. MEASUREMENTS OF THE (011) G-TYPE REFLECTION

Although the magnetic environment in our diffraction experiment constrains the portions of reciprocal space that we can access, we were able to also probe a limited region around the G-type reflection (0,1,1). In a field  $H\parallel c=2\text{T}$  we observe incommensurate reflections below 3.5K with the same incommensurability  $\epsilon$  and temperature dependence as for the satellites around the A-type (0,0,1) reflection (see Fig. S1 in the supplementary information). The commensurate (0,1,1) G-type reflection observed above 3.5 K arises only from the Fe-spin ordering (see Fig. 1). The fact that the intensity of the commensurate reflection does not vary through this transition suggests that the Fe order is not significantly perturbed, in agreement with our theory.

## III. DIELECTRIC MEASUREMENTS

Measurements of the capacitance and loss were performed both as a function of temperature between 0.3 and 15 K in field cooled mode and isothermally as a function of magnetic field up to 1.9 T, in zero field cooled mode. In our measurements, a calibrated Cernox resistance thermometer (CX-1030) on the sample holder was used to monitor the sample temperature, which was measured with an LakeShore 370 AC Resistance Bridge. The resolution of the temperature measurement is  $5 \cdot 10^{-4}$ , although the temperature stability decreases around 3 K, due to the boiling temperature of liquid  $^3\text{He}$  of 3.2 K. The capacitance and loss measurements were performed at a frequency of 1000 Hz and an excitation of 15 V. The resolution of the capacitance measurement is  $2 \cdot 10^{-5}$ .

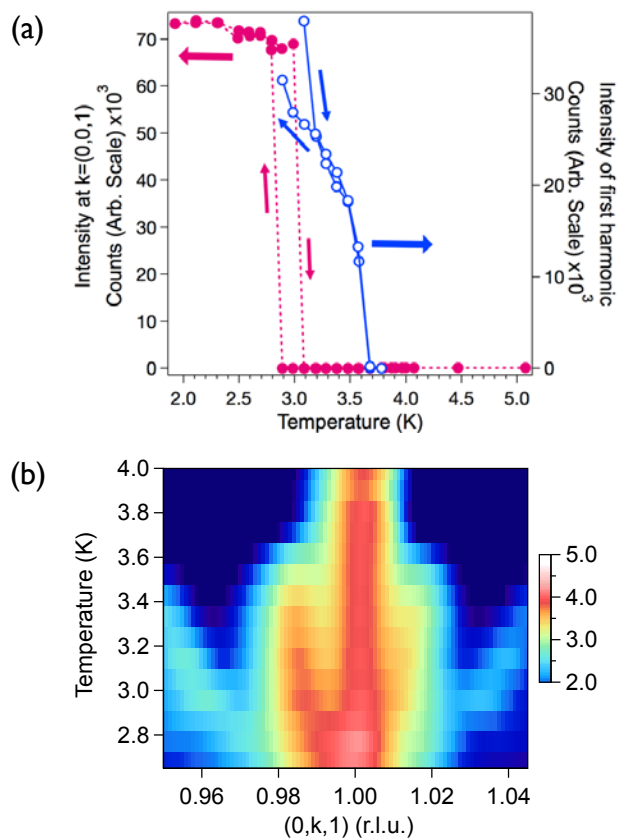


Fig. S1: **a**, Temperature dependence as a function of temperature of the A-type (0,0,1) reflection and the 1st harmonic reflection of the IC phase, determined from the neutron diffraction data in a magnetic field of 2 T applied along the *c*-axis. **b**, Single crystal neutron diffraction data measured on cooling and in a magnetic field parallel to the *c*-axis of  $H||c=2$  T. Scans are measured in reciprocal space along (0,*k*,1) around the G-type reflection (0,1,1). As above the temperature dependent neutron diffraction measurements are represented in a two-dimensional plot with intensity depicted as colour on a log scale shown on the right of the panel. The 1st and 3rd harmonic reflections are evident below 3.4 K.

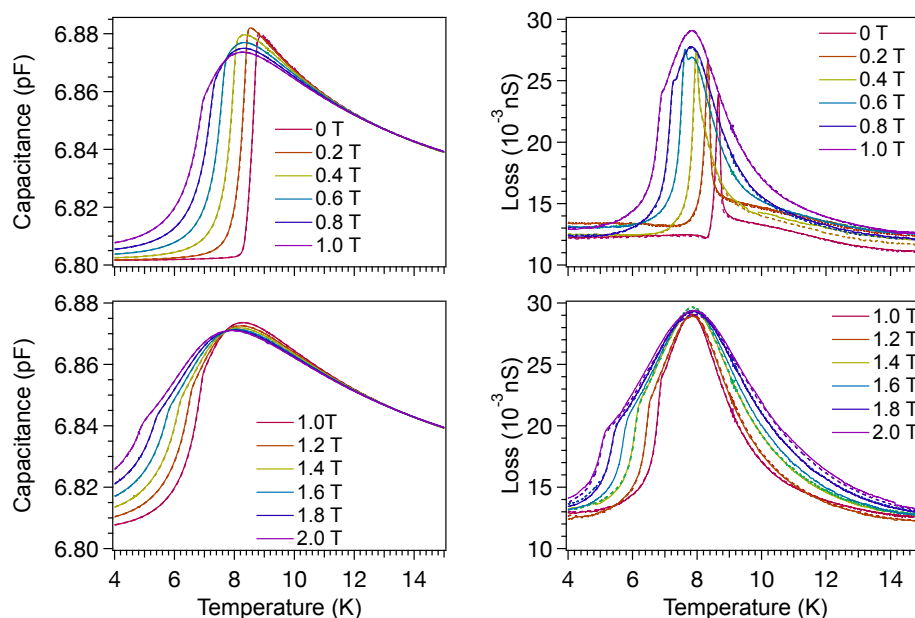


Fig. S2: Example data of capacitance and loss measured from a single crystal of  $\text{TbFeO}_3$  between 0 and 2 T as a function of temperature between 4 and 15 K, with data collected both on cooling (dashed line) and on warming (continuous line). In the data shown, no significant hysteresis is observed. Here the sample was cooled with an applied magnetic field and measurements were taken continuously during warmup with a sweep rate of 125 mK per minute while the field was maintained. Similar procedures were followed for these capacitance and loss measurements. We found that measurement on cooling showed exactly the same behaviour. We also noted that that measurements after field cooling and zero field cooling do not differ in this temperature range.

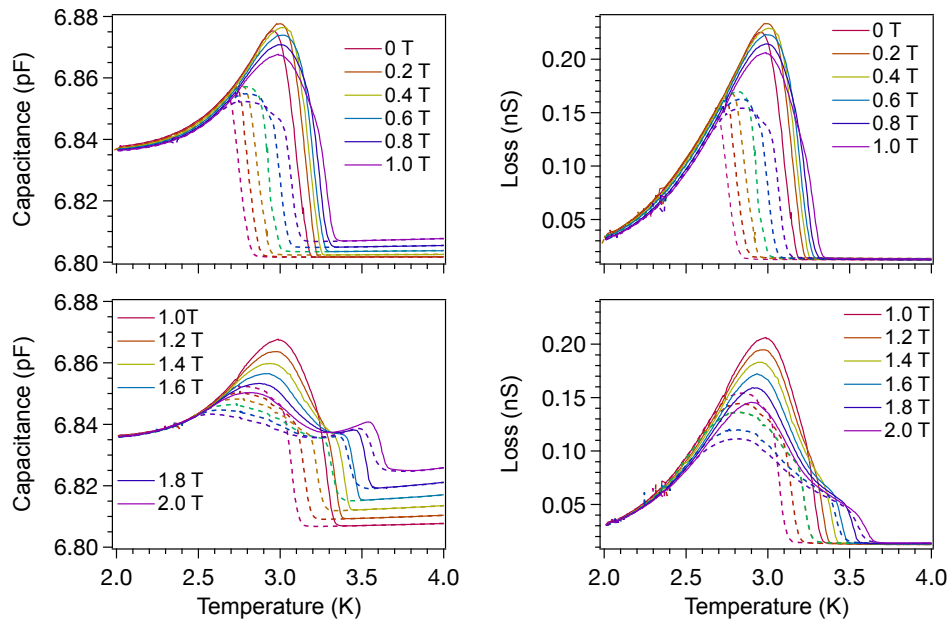


Fig. S3: Example data of capacitance and loss measured from a single crystal of  $\text{TbFeO}_3$  between 0 and 2 T as a function of temperature between 2 and 4 K, with data collected both on cooling (dashed line) and on warming (continuous line). Here the sample was cooled with an applied magnetic field while measurements were taken continuously during warming with a sweep rate of 30 mK per minute. Measurements were also performed down to 0.3 K, but no anomalies were found indicating the absence of further transitions.

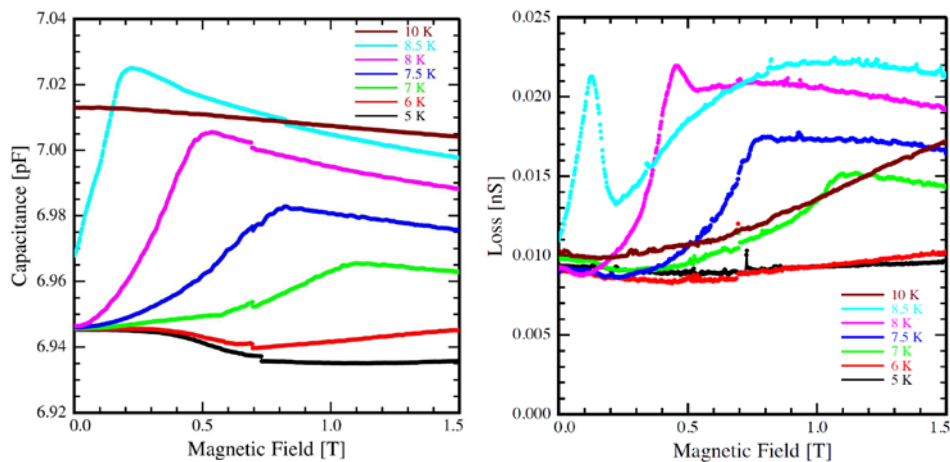


Fig. S4: Example data of capacitance and loss measured from a single crystal of  $\text{TbFeO}_3$  as a function of magnetic field between 5 and 10 K and up to 1.5 T. The sweep rate of the magnetic field used here was 50 mT per minute. Measurements were taken isothermally after zero field cooling.

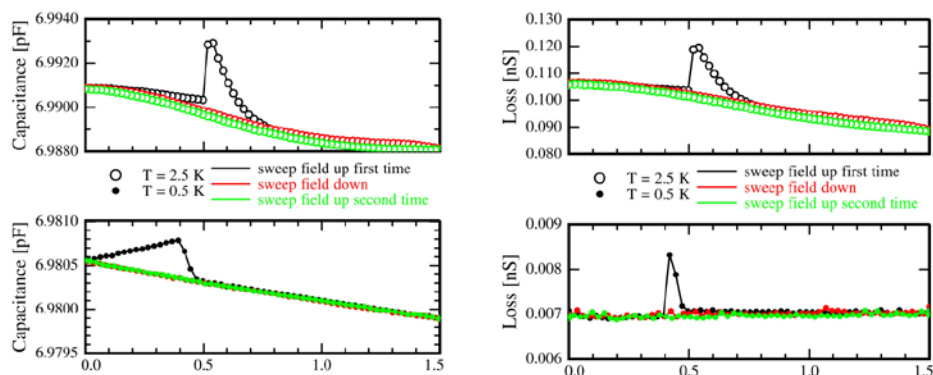


Fig. S5: Example data of the capacitance and loss measured at 0.5 and 2.5 K up to 1.5 T. A clear peak is observed for data measured after zero field cooling at 0.5 T, consistent with the transition from the LT phase to the LT' phase observed using neutron diffraction. The same peak is not observed when the field was ramped down from 1.5 T and neither is it found if we ramp the field up again. This behaviour was consistent for a series of measurements between 0.3 to 2.5 K and suggests that over this temperature range the LT' phase once entered into with field, is stable down to zero field. The sweep rate of the magnetic field for these measurements was 50 mT per minute.